

Lattice QCD Calculations of Hadron Structure: Status and Perspectives

Philipp HÄGLER

*Institut für Theoretische Physik T39, TU München, James-Franck-Strasse,
D-85747 Garching, Germany**)

The last years have seen significant advances in hadron structure calculations in lattice QCD. While extrapolations to the physical point and direct comparisons with experiment are still very challenging, lattice calculations provide already very valuable insights into a number of fundamental physics questions related to, e.g., the distribution of charge and momentum inside hadrons and the nucleon spin structure. To illustrate the recent achievements, we present and discuss latest lattice results for a small number of observables related to nucleon form factors and generalized parton distributions. We also present a study of the decomposition of the nucleon spin $1/2$ in terms of quark spin and orbital angular momentum contributions. We briefly discuss results and limitations of the relevant chiral fits and extrapolations.

§1. Introduction

Remarkable insights into the inner structure of hadrons have been provided during the last decades by countless theoretical, phenomenological and experimental studies. Complementary to these efforts, calculations from first principles in the framework of lattice QCD represent a highly promising approach to a wide range of fundamental hadron properties. In this contribution, we concentrate on a small number of results from recent dynamical lattice QCD studies. For more detailed accounts of the advances that have been made on the lattice, in particular with respect to the quark and gluon structure of the pion and the nucleon, we refer to 1)–6). We begin with an overview of lattice results for the Dirac mean square radius and the nucleon anomalous magnetic moment, including a brief discussion of corresponding predictions from heavy baryon chiral perturbation theory (HBChPT). This is followed by a presentation of moments of generalized parton distributions (GPDs) obtained by the LHP collaboration. The impact of these lattice results on the decomposition of the nucleon spin in terms of spin- and orbital angular momentum contributions is discussed in the final section, where lattice values for the up- and down-quark angular momentum will also be compared to other experimental, phenomenological and model studies.

Due to space limitations, we point the interested reader to Refs. 7) and 8) for a first exploratory lattice study of transverse momentum dependent distributions (TMDs) that already provided interesting insights into non-trivial correlations between spin- and momentum degrees of freedom for polarized quarks in a polarized nucleon.

*) Current address: Institut für Theoretische Physik, Universität Regensburg, D-93040 Regensburg, Germany

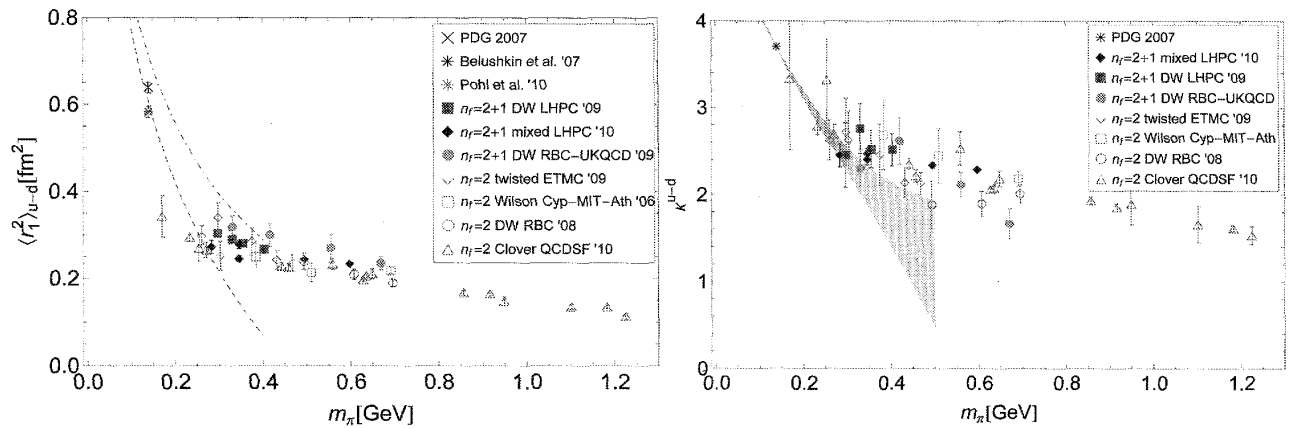


Fig. 1. Overviews of results for the isovector Dirac mean square radius (left) and the isovector anomalous magnetic moment (right) obtained by different lattice collaborations. The dashed lines and the shaded band represent predictions and fits based on (SSE-)HBChPT as described in the text. References are provided in the text.

§2. Dirac and Pauli form factors

Significant progress has been made during the recent years in dynamical lattice QCD calculations of the Dirac and Pauli nucleon form factors, $F_1(Q^2)$ and $F_2(Q^2)$, by a number of collaborations,^{9)–15)} with pion masses as low as ≈ 300 MeV. Very recently, QCDSF/UKQCD presented result for $N_f = 2$ Wilson fermions reaching down to $m_\pi \approx 180$ MeV¹⁶⁾ (albeit with larger statistical uncertainties at the lowest pion mass). Fundamental observables derived from the form factors are the mean square radii, $\langle r^2 \rangle_{1,2} \propto -(dF_{1,2}(Q^2)/dQ^2)_{Q^2=0}$, as well as the anomalous magnetic moment, $\kappa = F_2(0)$. On the left in Fig. 1 we provide an overview of results for the isovector Dirac mean square radius $\langle r_1^2 \rangle_{u-d}$ as a function of the pion mass. Overall, it is encouraging to see that the lattice data points obtained by the different collaborations are in good agreement within the statistical errors. Interestingly, at this point there is no clear systematic difference visible between calculations with $N_f = 2$ and $N_f = 2 + 1$ flavors. Although the lattice values are slowly increasing towards smaller pion masses, they are still about a factor of two below the phenomenological values^{17)–19)} even at the lowest lattice pion masses of $m_\pi \approx 250$ MeV. Notwithstanding potential systematic uncertainties in particular due to the finite lattice volumes, this indicates that a strong chiral dynamics has to set in for $m_\pi < 200 \dots 250$ MeV, and chiral perturbation theory (ChPT) indeed predicts that $\langle r_1^2 \rangle$ rises as $\ln(m_\pi)$ in the chiral limit, as illustrated by the dashed HBChPT²⁰⁾ and dash-dotted small scale expansion (SSE)-curves.^{21),22)} It will be major challenge to numerically demonstrate the onset of the predicted logarithmic rise in lattice calculations at lower pion masses.

An overview of results for the anomalous magnetic moment in the isovector channel is displayed on the right in Fig. 1 as a function of the pion mass. As before, the lattice results obtained for the different actions and numbers of flavors mostly overlap within uncertainties. Despite the steady increase towards smaller pion masses, the lattice data points are still about 30% below the experimental value even at pion masses of ≈ 250 MeV. In a first attempt to understand this difference more quanti-

tatively, we have fitted the data below $m_\pi = 300$ MeV, including the experimental value, using results from HBChPT in the SSE approach,^{21),22)} as illustrated by the shaded band on the left in Fig. 1. Fixing the axial nucleon- Δ coupling to $c_A = 1.5$, and varying the isovector nucleon- Δ coupling between $c_V = -1.5, \dots, -3.5$ GeV⁻¹, we find a good description of the data points with a comparatively large value for the isovector anomalous magnetic moment in the chiral limit, $\kappa^{0,u-d} \sim 5.2, \dots, 5.4$. Using the low energy constants obtained from this fit in a similar SSE-fit to the Pauli radius $\langle r^2 \rangle_2$ it turns out, however, that the SSE HBChPT expansion for $\langle r^2 \rangle_2$ breaks down shortly above m_π^{phys} . This indicates that the range of applicability in m_π of ChPT for radii is rather limited (at least to the given order in this ChPT-approach), in particular in comparison to the anomalous magnetic moment discussed before. A possible explanation for this can be seen in the fact that radii are given by derivatives with respect to a small expansion parameter (Q^2) and therefore correspond to a lower order in the chiral expansion relative to, e.g., $\kappa = F_2(0)$.

§3. Moments of GPDs and the nucleon spin structure

Generalized parton distributions (GPDs)^{*)} provide a particularly successful framework for the investigation of hadron structure, that not only encompasses the well known hadron form factors and the PDFs, but that also provides a solid basis for the decomposition of the nucleon spin in terms of spin and (orbital) angular momentum contributions of quarks and gluons. According to 26), the nucleon spin can be given in terms of x -moments of the GPDs $H(x, \xi, t)$ and $E(x, \xi, t)$,

$$\begin{aligned} \frac{1}{2} &= \sum_{q,g} J_{q,g} = \sum_{q,g} \frac{1}{2} \int_{-1}^1 dx x \{ H^{q,g}(x, \xi, t) + E^{q,g}(x, \xi, t) \}_{t=0} \\ &= \sum_{q,g} \frac{1}{2} (A_{20}^{q,g}(t) + B_{20}^{q,g}(t))_{t=0}, \end{aligned} \quad (3.1)$$

where A_{20} and B_{20} are generalized form factors (GFFs) that will be discussed in greater detail below. It is important to keep in mind that the total angular momentum of quarks can be further decomposed in a manifestly gauge-invariant manner in terms of quark spin and orbital angular momentum contributions, $J_q = \Delta\Sigma_q/2 + L_q$.²⁶⁾

GPDs can be measured for example in deeply virtual Compton scattering employing QCD factorization, however their extraction from experimental data turns out to be very challenging. This holds in particular for their dependence on x at fixed ξ , and therefore also for the x -moments in the decomposition in Eq. (3.1). As it turns out, this is different in the framework of lattice QCD, which represents at least in principle a straightforward (but in practice also challenging) approach from first principles to the lowest x -moments of PDFs and GPDs.

Substantial progress in particular with respect to moments of GPDs has been made since the pioneering calculations by the LHPC and QCDSF collaborations in

*) For reviews, we refer to 23)–25).

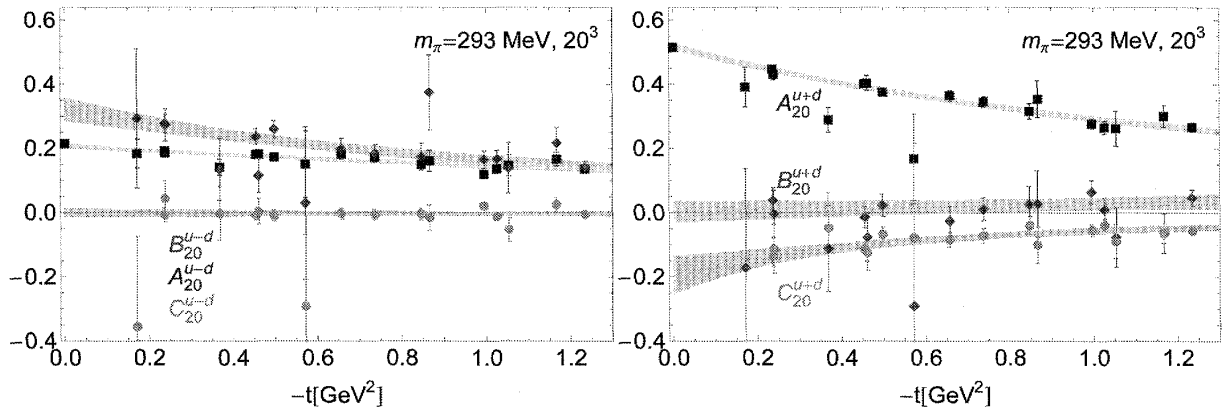


Fig. 2. Generalized form factors A, B, C as functions of the squared momentum transfer t , in the $\overline{\text{MS}}$ scheme at a scale of $\mu = 2$ GeV, for a pion mass of $m_\pi \approx 300$ MeV.³⁰⁾ The t -dependence can be parametrized by, e.g., a dipole ansatz, as illustrated by the shaded error bands.

2003.^{27),28)} A comprehensive lattice study of GPDs by LHPC using a mixed action approach was presented in 29). The discussions in the following sections will be based on a recent update of this study,³⁰⁾ which includes an additional ensemble at a lower pion mass of $m_\pi \approx 300$ MeV, a factor of 8 increased statistics, and a strongly improved statistical analysis.

The x -moments of generalized parton distributions can be written in terms of polynomials in powers of ξ with the GFFs as coefficients. For the $n=2$ -(x -)moments in the unpolarized case, the relevant GFFs A_{20}, B_{20}, C_{20} parametrize the off-forward matrix element of the (symmetric, traceless) energy momentum tensor, e.g. for quarks

$$\begin{aligned} \langle P' | \bar{q} \gamma^{\{\mu} D^{\nu\}} q | P \rangle = \langle P' | T_q^{\mu\nu} | P \rangle = \bar{U}(P') \left\{ \gamma^{\{\mu} \bar{P}^{\nu\}} A_{20}(t) - \frac{i \Delta_\rho \sigma^{\rho\{\mu} \bar{P}^{\nu\}}}{2m_N} B_{20}(t) \right. \\ \left. + \frac{\Delta^\mu \Delta^\nu}{m_N} C_{20}(t) \right\} U(P), \end{aligned} \quad (3.2)$$

where $\bar{P} = (P' - P)/2$, $\Delta = P' - P$, and $t = \Delta^2$. Examples of lattice results from LHPC³⁰⁾ for the t -dependence of these GFFs in the isovector and isosinglet channels are displayed in Fig. 2 for a comparatively low pion mass of ≈ 300 MeV. We notice at least two characteristic features: First, while the B_{20} -GFF is dominant in the isovector case, it is very small and fully compatible with zero within the uncertainties for all accessible values of t in the isosinglet channel. Conversely, the GFF C_{20} (which is directly related to the $n=2$ -moment of the so-called D -term³¹⁾) is zero within relatively small errors in the isovector channel, but clearly non-zero and negative for $u+d$ -quarks. From the sum of A_{20} and B_{20} at zero momentum transfer, we can compute the quark angular momentum J_q , cf. Eq. (3.1). The above findings for B_{20} obviously have a significant impact on the decomposition of the nucleon spin in terms of quark and gluon degrees of freedom.

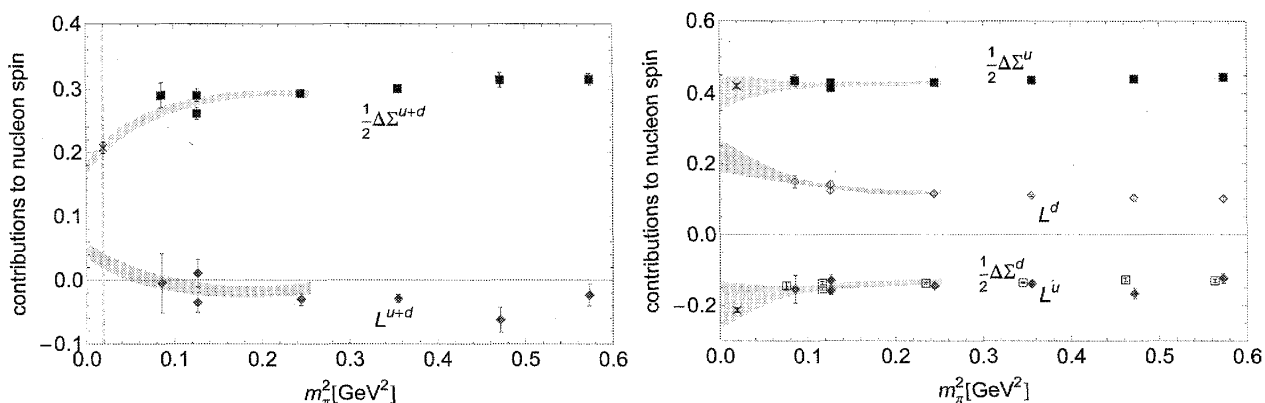


Fig. 3. Quark spin and OAM contributions to the nucleon spin $1/2$ in the $\overline{\text{MS}}$ scheme at a scale of $\mu = 2 \text{ GeV}$.³⁰⁾

§4. Decomposition of the nucleon spin

Instead of directly calculating the matrix elements of the gauge invariant quark OAM operator, we employ the relation $L_q = J_q - \Delta\Sigma_q/2$, together with corresponding results for the quark spin fraction $\Delta\Sigma_q$, to compute the OAM carried by the quarks. The numerical results for $u+d$ -quarks are shown on the left in Fig. 3 as a function of the squared pion mass. For the extrapolation of $\Delta\Sigma_{u+d}$ to the physical pion mass, we employed the heavy baryon ChPT results of (32). Although HBChPT at the given order is most probably not applicable at the accessible pion masses, the two-parameter fit to the lattice data points, indicated by the error band, shows an excellent (but likely accidental) agreement with the value from HERMES,³³⁾ indicated by the cross, at m_π^{phys} .

We used the results of a covariant baryon ChPT calculation³⁴⁾ for the simultaneous extrapolation of the GFFs A_{20}, B_{20}, C_{20} in m_π and in t , in particular to obtain $B_{20}(t=0, m_\pi^{\text{phys}})$. The results of the fits to the lattice data were subsequently used to compute $L_q = (A_{20}^q + B_{20}^q)_{t=0}/2 - \Delta\Sigma_q/2$, which is shown on the left in Fig. 3 for $q=u+d$ by the diamonds and the error band. Most remarkably, following this procedure, we find a very small OAM contribution of only $L_{u+d} \approx (6 \pm 3)\%$ of $1/2$ at the physical pion mass. Note that we obtain a slightly larger value, $L_{u+d} \approx (11 \pm 3)\%$, on the basis of a HBChPT extrapolation of J_{u+d} employing the results of (35). These results may be surprising and at first sight even appear to be in clear contradiction to expectations from relativistic quark models, where the quark OAM contributes about $\approx 30-40\%$ to the total nucleon spin. Moreover, it has been frequently pointed out in the past that non-zero quark orbital angular momentum is strictly required with respect to certain non-vanishing single spin asymmetries related to, e.g., the Sivers effect, as well as for the Pauli form factor $F_2(Q^2)$ to be non-zero.^{36)–39)}

Concerning the latter, it is important to be precise in the use of the term *quark orbital angular momentum*: The lattice results on the one hand correspond to the proton matrix element of the manifestly gauge invariant quark OAM operator as given in, e.g., Ref. 26), which is part of Jis nucleon spin sumrule, see Eq. (3.1) and the adjacent discussion. On the other hand, what is required with respect to a non-

vanishing $F_2(Q^2)$ and the Sivers effect are light cone wave functions with non-zero orbital angular momentum in an overlap representation of the corresponding matrix elements. Also, the more heuristic approach to explain single spin asymmetries, e.g. the Sivers effect, proposed in 38), requires a generically non-zero *quark orbital motion*. The notions of OAM and orbital motion in these contexts are, however, not necessarily in one-to-one correspondence with the gauge invariant L_q discussed before.

Furthermore, we note that L_q is in general not positive definite. To appreciate the potential consequences of this basic observation, it is useful to study the individual up and down quark OAM contributions to the nucleon spin, which are shown on the right in Fig. 3 as functions of m_π^2 , together with $\Delta\Sigma_{u,d}/2$ and the corresponding chiral extrapolations (given by the error bands). It indeed turns out that the orbital angular momentum of up and of down quarks is in each case *large* and of similar magnitude, but opposite in sign, and therefore nearly cancels in the sum over a wide range of pion masses. From the chiral extrapolations, we find that the individual quark OAM contributions are also substantial at the physical pion mass, amounting to $|L_{u,d}| \approx 33\%$. We also note that cancellations of this sort in the isosinglet channel are not unusual. A well known example is the anomalous magnetic moment, which is large both for the proton and for the neutron, $\kappa_p = F_2^p(0) \sim 1.79$ and $\kappa_n = F_2^n(0) \sim -1.91$, respectively. Using isospin symmetry, however, one finds that the sizeable, individual contributions from up and down quarks to κ_p largely cancel out in the sum, $\kappa_p^{u+d} \approx -0.36$. Keeping in mind that $F_2(Q^2 = -t)$ correspond to the first, and the GFF $B_{20}(t)$ to the second x -moment of the GPD $E(x, \xi=0, t)$, we also find this to be perfectly consistent with the results in Fig. 2, where in particular $B_{20}^{u+d}(t) \approx 0$, while $B_{20}^{u-d}(t)$ is large and positive.

We now briefly comment on the apparent discrepancy between the common expectations from relativistic quark model calculations that $L_{u+d} \approx 30 - 40\%$, and the lattice QCD result of a nearly vanishing total quark OAM, $L_{u+d} \approx 0$. As has been pointed already out some time ago,^{40),41)} the model calculations generically correspond to a low hadronic scale $\ll 1$ GeV, while a typical renormalization scale for which the lattice results are given is $\mu \sim 2$ GeV (e.g. in the $\overline{\text{MS}}$ -scheme). Since OAM is a scale and scheme dependent quantity,⁴²⁾ a naive, direct comparison of lattice and model values at the respective scales is therefore in general meaningless. In practice, based on LO and NLO QCD evolution, it indeed turns out that the scale dependence of quark OAM can be very strong at low scales,^{*}) and even lead to a change in sign for, e.g., L_{u-d} , as one goes down from larger scales to low hadronic scales.^{30),40),41)} A detailed comparison of improved model calculations with results from lattice QCD will be given in 43).

Finally, we show a comparison of the results for the total quark angular momentum $J_q = (A_{20}^q + B_{20}^q)_{t=0}/2$, as obtained from the chiral extrapolations of A_{20} and B_{20} mentioned above, with earlier lattice as well as model- and phenomenological calculations in Fig. 4 in the J_u, J_d -plane. It turns out that the numerical values,³⁰⁾

^{*}) Keeping in mind that the evolution equations in QCD perturbation theory might not be quantitatively applicable at the low scales.

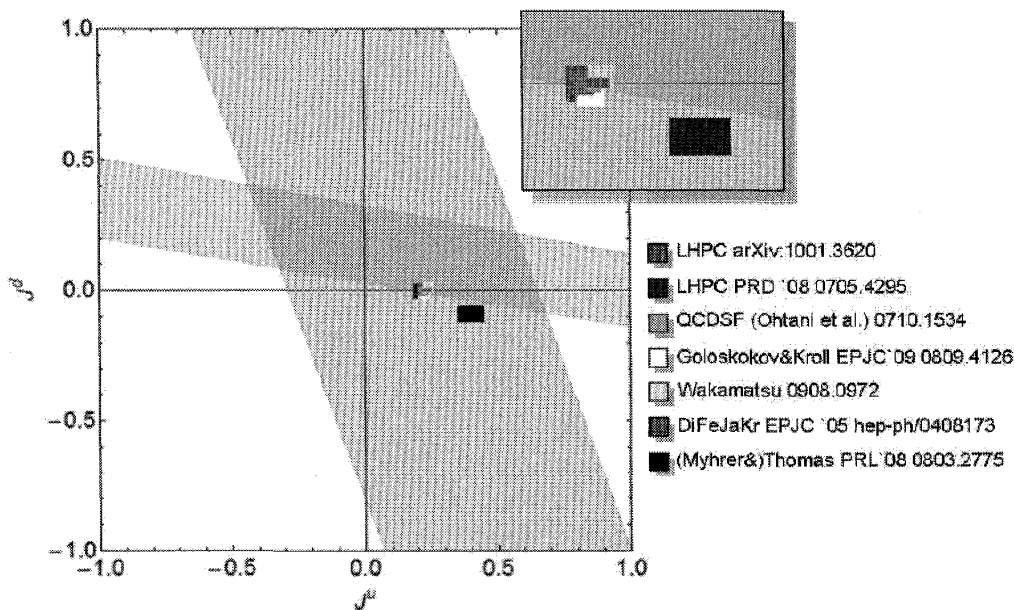


Fig. 4. Comparison of quark angular momentum contributions to the nucleon spin, obtained from different lattice (for systematic uncertainties, see footnote in this page), model and phenomenological studies,^{(11), (29), (41), (44)–(46)} displayed in the J_u, J_d -plane in the style of Refs. 47) and 48), for the $\overline{\text{MS}}$ scheme at a scale of $\mu = 2$ GeV. Note that the shaded bands are mainly given for illustration purposes and only approximately represent the constraints obtained in Refs. 47) and 48), which are still strongly model dependent.

$J_u = 0.236(6)$ and $J_d = 0.0018(37)$, are in surprisingly good agreement not only with the previous lattice computations, but also with most of the phenomenological and model results, at least when they are evolved to the common renormalization point of 4 GeV^2 . We note in passing that in the lattice calculations, the smallness of J_d can be traced back to a cancellation of the separately sizeable spin- and OAM contributions of down quarks, as can be inferred directly from the plot on the right in Fig. 3. It will be very interesting to see if the slight discrepancy to the cloudy bag model (CBM) study of Ref. 41) is due to systematic effects, missing contributions or similar on the side of the lattice^{*)} and the other approaches, or if it points towards the need for a further improvement of the CBM calculation.

Acknowledgements

It is a pleasure to thank M. Altenbuchinger, B. Musch, W. Weise and the colleagues from QCDSF/UKQCD and LHPC for successful collaboration. I gratefully acknowledge the support by the DFG Emmy-Noether program, cluster of excellence “Origin and Structure of the Universe”, and Sonderforschungsbereich/Transregio 55.

^{*)} Most notable issues are: discretization and finite volume effects, missing disconnected contributions, and the so far neglected mixing of quark and gluon operators under renormalization and evolution in the singlet sector.

References

- 1) K. Orginos, PoS(LAT2006)018.
- 2) P. Hägler, PoS(LATTICE 2007)013, arXiv:0711.0819.
- 3) J. M. Zanotti, PoS(LATTICE 2008)007, arXiv:0812.3845.
- 4) A. Schäfer, Nucl. Phys. A **805** (2008), 230c.
- 5) P. Hägler, Phys. Rep. **490** (2010), 49, arXiv:0912.5483.
- 6) D. B. Renner, arXiv:1002.0925.
- 7) P. Hägler et al., Europhys. Lett. **88** (2009), 61001, arXiv:0908.1283.
- 8) B. Musch et al., *MENU 2010 proceedings* (2010).
- 9) C. Alexandrou et al., Phys. Rev. D **74** (2006), 034508, hep-lat/0605017.
- 10) M. Göckeler et al. (QCDSF Collaboration), arXiv:0709.3370.
- 11) J. D. Bratt et al., PoS(LATTICE 2008)141, arXiv:0810.1933.
- 12) H.-W. Lin et al., Phys. Rev. D **78** (2008), 014505, arXiv:0802.0863.
- 13) T. Yamazaki et al., Phys. Rev. D **79** (2009), 114505, arXiv:0904.2039.
- 14) S. N. Syritsyn et al., Phys. Rev. D **81** (2010), 034507, arXiv:0907.4194.
- 15) C. Alexandrou et al., PoS(LAT2009)145, arXiv:0910.3309.
- 16) D. Pleiter et al. (QCDSF/UKQCD Collaboration), PoS(Lattice 2010)153.
- 17) M. A. Belushkin, H. W. Hammer and U. G. Meissner, Phys. Rev. C **75** (2007), 035202, hep-ph/0608337.
- 18) C. Amsler et al. (Particle Data Group), Phys. Lett. B **667** (2008), 1.
- 19) R. Pohl et al., Nature **466** (2010), 213.
- 20) V. Bernard et al., Nucl. Phys. B **388** (1992), 315.
- 21) T. R. Hemmert and W. Weise, Eur. Phys. J. A **15** (2002), 487, hep-lat/0204005.
- 22) M. Göckeler et al. (QCDSF Collaboration), Phys. Rev. D **71** (2005), 034508, hep-lat/0303019.
- 23) K. Goeke, M. V. Polyakov and M. Vanderhaeghen, Prog. Part. Nucl. Phys. **47** (2001), 401, hep-ph/0106012.
- 24) M. Diehl, Phys. Rep. **388** (2003), 41, hep-ph/0307382.
- 25) A. V. Belitsky and A. V. Radyushkin, Phys. Rep. **418** (2005), 1, hep-ph/0504030.
- 26) X.-D. Ji, Phys. Rev. Lett. **78** (1997), 610, hep-ph/9603249.
- 27) P. Hägler et al. (LHPC and SESAM Collaborations), Phys. Rev. D **68** (2003), 034505, hep-lat/0304018.
- 28) M. Göckeler et al. (QCDSF Collaboration), Phys. Rev. Lett. **92** (2004), 042002, hep-ph/0304249.
- 29) P. Hägler et al. (LHPC Collaboration), Phys. Rev. D **77** (2008), 094502, arXiv:0705.4295.
- 30) J. D. Bratt et al. (LHPC), Phys. Rev. D **82** (2010), 094502, arXiv:1001.3620.
- 31) M. V. Polyakov and C. Weiss, Phys. Rev. D **60** (1999), 114017, hep-ph/9902451.
- 32) M. Diehl, A. Manashov and A. Schäfer, Eur. Phys. J. A **31** (2007), 335, hep-ph/0611101.
- 33) A. Airapetian et al. (HERMES Collaboration), Phys. Rev. D **75** (2007), 012007.
- 34) M. Dorati, T. A. Gail and T. R. Hemmert, Nucl. Phys. A **798** (2008), 96, nucl-th/0703073.
- 35) J.-W. Chen and X.-D. Ji, Phys. Rev. Lett. **88** (2002), 052003, hep-ph/0111048.
- 36) S. J. Brodsky, et al., Nucl. Phys. B **593** (2001), 311, hep-th/0003082.
- 37) S. J. Brodsky, D. S. Hwang and I. Schmidt, Phys. Lett. B **530** (2002), 99, hep-ph/0201296.
- 38) M. Burkardt, Phys. Rev. D **66** (2002), 114005, hep-ph/0209179.
- 39) M. Burkardt and D. S. Hwang, Phys. Rev. D **69** (2004), 074032, hep-ph/0309072.
- 40) M. Wakamatsu and Y. Nakakoji, Phys. Rev. D **77** (2008), 074011, arXiv:0712.2079.
- 41) A. W. Thomas, Phys. Rev. Lett. **101** (2008), 102003, arXiv:0803.2775.
- 42) X.-D. Ji, J. Tang and P. Hoodbhoy, Phys. Rev. Lett. **76** (1996), 740, hep-ph/9510304.
- 43) M. Altenbuchinger, P. Hägler and W. Weise, in preparation, 2010.
- 44) D. Brömmel et al. (QCDSF-UKQCD Collaboration), PoS(LATTICE 2007)158, arXiv:0710.1534.
- 45) M. Wakamatsu, Eur. Phys. J. A **44** (2010), 297, arXiv:0908.0972.
- 46) M. Diehl et al., Eur. Phys. J. C **39** (2005), 1, hep-ph/0408173.
- 47) A. Airapetian et al. (HERMES Collaboration), J. High Energy Phys. **06** (2008), 066, arXiv:0802.2499.
- 48) M. Mazouz et al. (Jefferson Lab Hall A Collaboration), Phys. Rev. Lett. **99** (2007), 242501, arXiv:0709.0450.